Multi-Axis Attitude Maneuver of a Flexible Spacecraft Using Adaptive Hybrid Sliding Mode Control

M. Kabganian [§]; M. Shahravi[†]; and A. Alasty[‡]

ABSTRACT

A new control strategy for attitude maneuver of an elastic spacecraft is presented. Adaptive sliding mode control scheme with a synthesized Hybrid Sliding Surface (HSS) is used to overcome the difficulties arising from measurement of flexible dynamics coordinates. The excitation of flexible modes that frequently happens in the conventional sliding mode is minimized by using the synthesized sliding surface. The model of the spacecraft considered as rigid central hub and two flexible appendages. Collocated actuators and sensors are placed on the rigid central hub. Stability proof of the overall closed-loop system is given via Lyapunov analysis. Asymptotical tracking control of the multi-axis attitude motion and suppression of the elastic deformations are accomplished. Numerical simulations show the effectiveness of the proposed control scheme.

KEYWORDS

Attitude Control, Flexible Spacecraft, Adaptive Sliding Mode, Hybrid Sliding Surface

1. INTRODUCTION

During the past few decades, control problems for flexible space structures have received significant attention because of the important demands for low-energy consumption and limitation of mass. Since the control degree of freedom is much fewer than the motion degree of freedom when a flexible structure is commanded to track a desired trajectory, many control strategies that succeed in conventional rigid systems can not be directly applied to control of flexible systems.

Flexible structures are infinite dimensional systems due to the flexibility inherent in the structures. The equations of motion of the infinite dimensional systems are usually described by Partial Differential Equations (PDE) and the limited dimensions of practical controllers often requires discretization of original PDE model into a system of finite dimensional Ordinary Differential Equations (ODE). Modeling errors are always introduced when the Reduced Order Models (ROM) are used. On the other hand, the implementations of the most control strategies that have been reported in the literatures are not simple since the control laws involve knowledge of the flexible dynamics states. Therefore, the design of robust and practical controllers to accommodate modeling errors such as spill-over effects due to the unmodeled dynamics and uncertainties and difficulties arising from obtaining data for flexible dynamics coordinates is a challenging task and still under investigation.

In recent years, several studies related to the control of flexible space systems have been done, and linear and nonlinear control systems have been designed. An excellent survey of research in this area has been published by Hyland *et al.*, which provides a good source of references [1]. Optimal controllers for linear and nonlinear models of flexible space structures have been designed [2, 3]. Lyapunov stability theory has been used to design controllers for the maneuver and vibration control of space vehicle [4,5]. A perturbation method in order to separate large and small motion has been used to obtain a feedback controller [6]. An input shaping method that adjusts the input command to the actuators so that the excitation of the flexible modes being minimized has been used [7,8].

In these studies, it is assumed that the dynamics of the space structures are exactly known. In the presence of uncertainty, adaptive and sliding mode control systems have been designed [9-13]. However, conventional

[§] M. Kabganian is with the Department of Mechanica Engineering, Amirkabir University of Technology, Tehran, Iran (e-mail: kabgan@aut.ac.ir).

[†] M. Shahravi is with the Department of Mechanica Engineering, Amirkabir University of Technology, Tehran, Iran (e-mail: shahravi@aut.ac.ir).

[‡] A. Alasty is with the Department of Mechanica Engineering, Sharif University of Technology, Tehran, Iran (e-mail: aalasty@sharif.edu).

adaptive controllers, are suitable only for parameter uncertainties. On the other hand, the derivation of the sliding mode control systems requires knowledge of the bounds on the uncertainties. Also, the conventional sliding mode designed in the time domain is hardly applicable as the inherent elastic modes of the flexible systems will be unduly excited by the switching control input.

In this paper, an adaptive sliding mode control with a synthesized HSS is used to overcome these drawbacks in the attitude control of a flexible spacecraft. Also, in the proposed controller, the measurement of the flexible modes is not required and due to the difficulties of the measurement of flexible dynamics coordinates, this is an eminent property for implementation of the controller.

In the following section, attitude dynamics formulation of the spacecraft has been derived. In sec. III, HSS and its characteristics have been introduced. The HSS and the Lyapunov technique have been used in sec. IV in order to design the control and adaptation laws. Numerical simulations in sec. V illustrate the performances of the proposed controller. A discussion of the presented results concludes the paper.

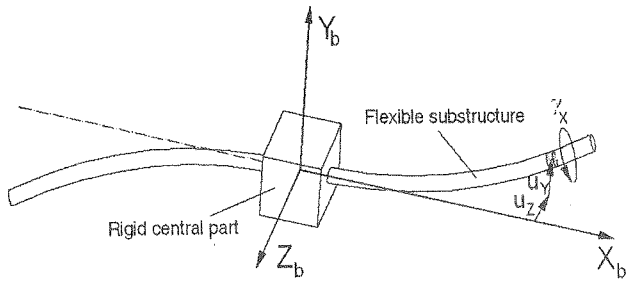

Figure 1: Flexible spacecraft model.

2. DYNAMIC MODEL

The mathematical model of the slewing flexible spacecraft can be derived by using the Assumed Mode Method (AMM) associated with Lagrangian formulation. As shown in Figure 1, a rigid central hub with two elastic appendages attached is considered as the model of the spacecraft. Two clamped loaded Euler-Bernoulli beams are selected to model the elastic deflections of flexible appendages in rotational motions. The spacecraft is controlled by a torquer on the rigid hub. When the spacecraft is maneuvered, the elastic members connecting to the hub, experience structural deformation. As shown in Figure 1, two flexural deflections in y and z directions ($u_y(x,t)$, $u_z(x,t)$) and one rotational deflection about x-axis ($\gamma_x(x,t)$), are considered for modeling the elastic deformations of the flexible substructures. The problem of interest here is to control the orientation of the main body of the spacecraft as well as to suppress elastic deformations.

The attitude dynamic model of the spacecraft can be obtained in the following form [6, 15]:

$$\begin{bmatrix} M_{rr} & M_{rf} \\ M_{fr} & M_{ff} \end{bmatrix} \begin{Bmatrix} \dot{\omega} \\ \ddot{q}_f \end{Bmatrix} + \begin{Bmatrix} h_r(\omega, q_f, \dot{q}_f) \\ h_f(\omega, q_f, \dot{q}_f) \end{Bmatrix} = \begin{Bmatrix} T_r \\ 0 \end{Bmatrix} \quad (1)$$

where $\omega = [\omega_x \quad \omega_y \quad \omega_z]$ is the angular velocity of the spacecraft with respect to the body frame $F_b(O_b X_b Y_b Z_b)$, q_f is the modal coordinate vector and T_r is the external torque vector acting on the central hub. Subscripts r and f denote rigid and flexible mode parts, respectively. The elements of sub matrices M and h are given in appendix A.

For derivation of the above equations, the elastic deformations of the appendages are considered to be:

$$^i u_y(x,t) = {}^i\psi_y^T(x)\ {}^i q_y(t) = \sum_{j=1}^{m} {}^i\psi_{yj}(x)\ {}^i q_{yj}(t) \quad (2)$$

$$^i u_z(x,t) = {}^i\psi_z^T(x)\ {}^i q_z(t) = \sum_{j=1}^{m} {}^i\psi_{zj}(x)\ {}^i q_{zj}(t) \quad (3)$$

$$^i \gamma_x(x,t) = {}^i\psi_\gamma^T(x)\ {}^i q_\gamma(t) = \sum_{j=1}^{m} {}^i\psi_{\gamma j}(x)\ {}^i q_{\gamma j}(t) \quad (4)$$

where x is the coordinate of any point along the undeformed member, $^i\psi_{yj}(x)$, $^i\psi_{zj}(x)$ and $^i\psi_{\gamma j}(x)$ are the jth assumed mode shape function for each elastic displacement of the ith substructure, $^i q_{yj}$, $^i q_{zj}$ and $^i q_{\gamma j}$ are the jth generalized coordinates for ith substructure so that $q_f = \left[{}^1q_y \quad {}^1q_z \quad {}^1q_\gamma \middle| {}^2q_y \quad {}^2q_z \quad {}^2q_\gamma\right]^T$ and m is the total number of elastic modes retained in the discrete model [4].

3. HYBRID SLIDING SURFACE (HSS)

Sliding mode control has received a good deal of attention because of its robustness and simplicity. Successful applications to practical systems are numerous. However, the conventional sliding mode designed in the time domain is hardly applicable to control of flexible systems as the inherent resonance modes of the systems will be unduly excited by switching control input. To solve this problem, Xu and Cao [16] have proposed a new sliding surface that obtained suitable transient and steady state dynamics whereas flexible modes are being minimally excited. In this paper, it is used and combined with an adaptive scheme to control the flexible spacecraft in attitude maneuver in order to overcome uncertainties, disturbances and difficulties arising from measurement of flexible dynamics coordinates.

The HSS is proposed as

$$S_H = \alpha S_{FSOSM} + (1-\alpha) S_{TSM} \quad (5)$$

where the subscripts FSOSM and TSM indicate Frequency Shaped Optimal Sliding Mode and Terminal Sliding Mode, respectively. The weighing coefficient α should be chosen properly to obtain requested performance and satisfy stability conditions.

Supposing e_1 and e_2 to be tracking error and its

time derivative, respectively, the FSOSM obtained with augmenting the system $e_2 = \dot{e}_1$ with the following second-order high-pass filter

$$F(s) = \left(\frac{a s + \omega_c}{s + \omega_c} \right)^2 \tag{6}$$

The corner frequencies of the filter are $(1/a)\omega_c$ and ω_c where $a>1$ and $\omega_c>1$ *rad/s*. The sliding surface could be derived as [17]:

$$S_{FSOSM} = e_2 + c_e e_1 + c_1 z_1 + c_2 z_2 = 0 \tag{7}$$

where z_1 and z_2 are the state-space representation of the filter and c_e, c_1 and c_2 are constants and can be obtained from an optimization procedure.

The TSM sliding surface has been proposed by Zak [18] as:

$$S_{TSM} = e_2 + c_p e_1^p = 0 \tag{8}$$

where

$$\begin{aligned} p &= p_1/p_2 \\ p_1 &= 2m_1 + 1 \qquad , m_1 = 0,1,2,... \\ p_2 &= 2m_2 + 1 \qquad , m_2 = 1,2,3,... \end{aligned} \tag{9}$$

Using equations (5), (7) and (8), the HSS can be obtained as:

$$S_H = e_2 + \alpha c_e e_1 + (1-\alpha) c_p e_1^p + \alpha c_1 z_1 + \alpha c_2 z_2 \tag{10}$$

This synthesized sliding surface has following characteristics that make it reasonable to use for controlling the flexible systems:

i) The equivalent switching slope is:

$$\frac{\partial S_H}{\partial e_1} = \alpha c_e + c_p (1-\alpha) p e_1^{p-1} \tag{11}$$

At the initial stage, when the tracking error is large, the sliding surface is dominated by the FSOSM part, which can avoid exciting the elastic modes of the system. It may be obtained by setting sufficiently large α (no more than stability bound). As the tracking error decreases, the switching slope increases and expedites convergence.

ii) In the practical implementations, the system samples the controller's output and plant's output at the limited sampling rates. The limited sampling rates cause the actual system states to be in the neighborhood of the sliding surface. Suppose that γ is the bound of the neighborhood. the extremal steady state error can be derived to be:

$$e_{ss} = \left[\frac{\gamma}{(1-\alpha) c_p} \right]^{1/p} \tag{12}$$

For comparison, the extremal steady state error of a conventional sliding surface $S_{conv} = e_2 + c e_1 = 0$, can be derived to be γ/c. As $1/p>1$ and usually $\gamma/(1-\alpha)<1$, $e_{ss} < \gamma/c$. Hence the HSS reduces steady state error.

iii) The additional states introduced by the high-pass filter in the FSOSM part of the surface, offer additional degrees of freedom in the sliding mode control design. Given the initial values $e_1(t_0)$ and $e_2(t_0)$, $z_1(t_0)$ and $z_2(t_0)$ can be chosen to eliminate the reaching phase, *i.e.*

$$\begin{aligned} e_2(t_0) + \alpha c_e e_1(t_0) + (1-\alpha) c_p (e_1(t_0))^p \\ + \alpha c_1 z_1(t_0) + \alpha c_2 z_2(t_0) = 0 \end{aligned} \tag{13}$$

Since the sliding mode exists from the very beginning, the system is more robust against perturbations than the other sliding mode control scheme with reaching phase.

4. ADAPTIVE SLIDING MODE CONTROL LAW

The Euler parameters (quaternions) are chosen to describe the attitude kinematics of the spacecraft. They have the advantage of being well defined for the whole range for attitude motions. Introducing $\boldsymbol{\beta}_d$ as desired attitude, the hybrid sliding surface may be developed as:

$$\boldsymbol{S}_H = \boldsymbol{\omega} + \alpha \boldsymbol{c}_e \boldsymbol{e}_r + (1-\alpha) \boldsymbol{c}_p \, \mathrm{g}(\boldsymbol{e}_r) + \alpha \boldsymbol{H} \boldsymbol{z} \tag{14}$$

where

$$\boldsymbol{e}_r = \boldsymbol{\beta} - \boldsymbol{\beta}_d \tag{15}$$

$$\boldsymbol{c}_e = diag(c_{e1} \quad c_{e2} \quad c_{e3}) \tag{16}$$

$$\boldsymbol{c}_p = diag(c_{p1} \quad c_{p2} \quad c_{p3}) \tag{17}$$

$$\mathrm{g}(\boldsymbol{e}_r) = [\mathrm{g}(e_{r1}) \quad \mathrm{g}(e_{r2}) \quad \mathrm{g}(e_{r3})]^T \tag{18}$$

$$\mathrm{g}(e_{rk}) = \begin{cases} e_{rk}^p & |e_{rk}| > \varepsilon_k \\ p \varepsilon^{p-1} e_{rk} & |e_{rk}| \le \varepsilon_k \end{cases} \tag{19}$$

$$\boldsymbol{H} = \begin{bmatrix} c_{z11} & c_{z12} & 0 & 0 & 0 & 0 \\ 0 & 0 & c_{z21} & c_{z22} & 0 & 0 \\ 0 & 0 & 0 & 0 & c_{z31} & c_{z32} \end{bmatrix} \tag{20}$$

$$\boldsymbol{z} = [z_{11} \quad z_{12} \quad z_{21} \quad z_{22} \quad z_{31} \quad z_{32}]^T \tag{21}$$

c_{ek}, c_{pk} and c_{zk} are coefficients of the sliding surface and ε_k are some small positive constants, for k=1,2,3. The vector $\boldsymbol{z}$ includes states of three second-order high-pass filters *F(s)*. The state-space representation of the filters can be obtained as:

$$\dot{\boldsymbol{z}} = \boldsymbol{A}\boldsymbol{z} + \boldsymbol{B}\dot{\boldsymbol{e}}_r \tag{22}$$

where

$$\boldsymbol{A} = \begin{bmatrix} 0 & 1 & 0 & 0 & 0 & 0 \\ -\omega_{1c}^2 & -2\omega_{1c} & 0 & 0 & 0 & 0 \\ 0 & 0 & 0 & 1 & 0 & 0 \\ 0 & 0 & -\omega_{2c}^2 & -2\omega_{2c} & 0 & 0 \\ 0 & 0 & 0 & 0 & 0 & 1 \\ 0 & 0 & 0 & 0 & -\omega_{3c}^2 & -2\omega_{3c} \end{bmatrix} \tag{23}$$

$$\boldsymbol{B} = \begin{bmatrix} 0 & 1 & 0 & 0 & 0 & 0 \\ 0 & 0 & 0 & 1 & 0 & 0 \\ 0 & 0 & 0 & 0 & 0 & 1 \end{bmatrix}^T \tag{24}$$

ω_{kc} for k=1,2,3 are the corner frequencies of the filters that must be chosen properly to prevent the excitation of elastic modes of the system. It can be obtained from equations (1) and (14) that

$$\dot{S}_H = \Delta^{-1}\left(T_r + W^T Y\right) \quad (25)$$

where

$$\Delta = M_{rr} - M_{rf} M_{ff}^{-1} M_{fr} \quad (26)$$

$$W = [W1 \quad W2 \quad W3 \quad W4 \quad W5]^T \quad (27)$$

$$Y = \left[Y1^T \quad Y2^T \quad Y3^T \quad Y4^T \quad Y5^T\right]^T \quad (28)$$

It is considered that the elements of matrix W be consisting of uncertainties and the elements of Y be measurable or definite. See appendix B for more details.

A variable structure control law for attitude tracking is introduced as:

$$T_r = -\mathrm{sgn}(S_H)\left(\hat{W}^T|Y| + \sigma\right) \quad (29)$$

where

$$\mathrm{sgn}(S_H) = diag[\mathrm{sgn}(S_{H1}) \quad \mathrm{sgn}(S_{H2}) \quad \mathrm{sgn}(S_{H3})] \quad (30)$$

$$\sigma = [\sigma_1 \quad \sigma_2 \quad \sigma_3]^T \quad , \sigma_k > 0 \text{ for } k=1,2,3 \quad (31)$$

$\hat{W}$ is the estimated value of W^* and $W_{ij}^* > |W_{ij}|$ for all values of q_f, $\dot{q}_f$ and other system parameters. In order to implement the controller, estimation of $\hat{W}_{ij}$ must be made. In practice, a suitable estimation for $\hat{W}_{ij}$ is difficult. Over estimation may result in unnecessary high gains and large chattering which degrade system performance. Underestimation, on the other hand is not permitted as it may lead to instability. To alleviate the difficulties arising from making conjectural data for flexible dynamic coordinates, parameter variations, disturbances and other system uncertainties, the following adaptation law is proposed:

$$\dot{\hat{W}} = \Gamma Y |S_H|^T \quad (32)$$

Γ is the adaptation gain and the initial value of the $\hat{W}$ can be set very small. The small value at the initial stage reduces the impact to the system. On the other hand, the increasing value of $\hat{W}$ when approaching the equilibrium, can lower steady state error.

It can be shown that the error dynamics resulting from the above control and adaptation laws are stable in the sense of Lyapunov. The details will be stated in the following theorem.

Theorem1: Let the control objective for the flexible spacecraft be to force the rigid body modes to follow some prespecified trajectories, while simultaneously damping out the elastic modes. Then, the control law (29) and adaptation law (32) can achieve this objective and ensures that S_H tends to zero as time tends to infinity.

Proof: Consider the following Lyapunov function candidate

$$V = \frac{1}{2}\lambda_{\max}(\Delta) S_H^T S_H + \frac{1}{2}\gamma^{-1} trace\left[\tilde{W}\tilde{W}^T\right] \quad (33)$$

where $\tilde{W} = \hat{W} - W^*$ is the estimation error and $\lambda_{\max}(\Delta)$ is the maximum eigenvalue of Δ. Taking the time derivative of V and using equations (25), (29) and (33), yields:

$$\begin{aligned}
\dot{V} &= \lambda_{\max}(\Delta) S_H^T\left[\Delta^{-1}\left(\tau + W^T Y\right)\right] \\
&\quad + \gamma^{-1} trace\left[\left(\dot{\hat{W}} - \dot{W}^*\right)\gamma |S_H| Y^T\right] \\
&= -\lambda_{\max}(\Delta) S_H^T \Delta^{-1} \hat{W} |Y| \mathrm{sgn}(S_H) \\
&\quad - \lambda_{\max}(\Delta) S_H \Delta^{-1} \sigma \,\mathrm{sgn}(S_H) \\
&\quad + \lambda_{\max}(\Delta) S_H^T \Delta^{-1} W^T Y \\
&\quad + trace\left[\hat{W}|S_H||Y|^T - W^*|S_H|Y^T\right] \\
&\le -|S_H|^T \hat{W}^T |Y| - |S_H|^T \sigma + S_H^T \lambda_{\max}(\Delta)\Delta^{-1} W^T Y \\
&\quad + |S_H|^T \hat{W}^T |Y| - |S_H|^T W^{*T} Y \\
&\le -|S_H|^T \sigma
\end{aligned} \quad (34)$$

Since the $V(t)$ is a continuous function and positive definite and its derivative is negative definite, it follows that V, $\lambda_{\max}$, S_H and $\tilde{W}$ are bounded and consequently $|Y|$, β, q_f and $\dot{S}_H$ are all bounded. Then using Barbalat's Lemma [19], one concludes that S_H tends to zero as time tends to infinity, which implies that the tracking error and its time derivative converge to zero as time tends to infinity.

The proposed control scheme has two potential problems. First, the adaptation law (32) is a positive integration process. In practical implementation, $S_H = 0$ can hardly be reached due to the presence of system perturbations and limited sampling rate. These residues in S_H, though small, will keep the adaptation integration going on and eventually lead to very high gains or even instability. The second problem is that the control law (29) is discontinuous crossing switching surface $S_H = 0$ due to the $\mathrm{sgn}(S_H)$ term. This characteristic may induce the undesirable chattering problem.

To overcome these drawbacks, we introduce the dead zone scheme to shut the adaptation mechanism off when the switching surface enters a sufficiently small bound and also replace the signum function by a saturation function in control law. The saturation boundary layer is chosen to be consistent with the dead zone. The revised control and adaptation schemes are given below:

$$T_r = -\mathrm{sat}(S_H)\left(\hat{W}^T|Y| + \sigma\right) \quad (35)$$

$$\dot{\hat{W}} = \begin{cases} \gamma Y |S_H| & S_H^T S_H > \delta^T \delta \\ 0 & S_H^T S_H \le \delta^T \delta \end{cases} \quad (36)$$

where

$$\delta = [\delta_1 \quad \delta_2 \quad \delta_3]^T \quad , \delta_k > 0 \quad \text{for } k=1,2,3 \quad (37)$$

is the size of deadzone and

$$\text{sat}(S_H,\delta)=diag[\text{sat}(S_{H1},\delta_1)\ \ \text{sat}(S_{H2},\delta_2)\ \ \text{sat}(S_{H3},\delta_3)]^T$$

$$\text{sat}(S_{Hk},\delta_k)=\begin{cases}\text{sgn}(S_{Hk}) & |S_{Hk}|>\delta_k \\ S_{Hk}/\delta_k & |S_{Hk}|\le\delta_k\end{cases} \quad k=1,2,3 \quad (38)$$

Theorem 2: The control law (35) and adaptation law (36) make the specified dead zone to be an attractive region and ensure that sliding surface can be reached in a finite time.

Proof: Define D_1 and D_2 as

$$D_1=\left\{\ t\middle|\ |S_H|>\delta\right\} \quad (39)$$

$$D_2=\left\{\ t\middle|\ |S_H|\le\delta\right\} \quad (40)$$

so that $D_1\cup D_2=R^+$. Consider the following Lyapunov function candidate

$$V=\begin{cases}\frac{1}{2}\lambda_{\max}(\Delta)S_H^TS_H+\frac{1}{2}\gamma^{-1}\,trace[\tilde{W}^T\tilde{W}] & t\in D_1 \\ \frac{1}{2}\lambda_{\max}(\Delta)\delta^T\delta+\frac{1}{2}\gamma^{-1}\,trace[\tilde{W}^T\tilde{W}] & t\in D_2\end{cases} \quad (41)$$

Note that V is a continuous function and $V\ge\frac{1}{2}\delta^T\delta>0$.

When $t\in D_1$, system states stay outside the dead zone and $|S_H|>\delta$. In term of (34);

$$\dot{V}\le-|S_H|\varepsilon\le-\delta^T\varepsilon<0 \quad (42)$$

This shows $\dot{V}$ is negative definite. Any system states lies outside the region will reach and enter it at some finite time. The total time during which adaptation takes place is finite. When $t\in D_2$ the system states lies inside the region and sliding condition is satisfied. This concludes the proofs.

The proposed control and adaptation laws have following properties:

i) The measurement of the flexible modes is not necessary. Due to difficulty of the measurement of q_f and $\dot{q}_f$, this is an eminent property for implementation of the controller

ii) In practice, a suitable estimation for W^* is difficult as we are not able to anticipate the variation bounds of uncertainties. Overestimation may result in unnecessarily high gains and large chattering which degrade system performance. Underestimation, on the other hand, is not permitted as it may lead to instability. The proposed adaptation law for estimating W^*, solve this problems and alleviate the difficulties arising from making conjectural data for flexible modes, parameter variations, disturbances and other system uncertainties.

iii) Setting W^* to be zero at the initial stage reduces the impact to the system at the start of the control process. On the other hand, the increasing of W^* when approaching the equilibrium can lower steady-state error.

iv) Using HSS, let to obtain favorite transient and steady state response without excitation of unwanted structural modes.

5. SIMULATION RESULTS

In this section, results of the numerical simulations for the closed-loop system are presented. Numerical values of the simulation parameters are given in Table 1. The first five flexible modes are retained in the model, thus m=5 . The lowest natural frequency of the system is obtained 5.12 *rad/s*. Then ω_c and a are chosen to be 2 *rad/s* and10 respectively. This ensures a 40 *db* roll-off rate for any frequency above ω_c that is lower than the first natural frequency of the system. Also, the coefficients c_{ek}, c_{zk1} and c_{zk2} for k=1,2,3 are calculated to be 0.01, -21.2183 and -4.8112, respectively. Considering the sampling period to be 1 *ms*, the numerical values of the c_{pk} and p are chosen to be 2 and 2/3 respectively and α is setting to be 0.9 . Hence the HSS is obtained as :

$$S_H=\omega+0.009U_{3\times3}\,e_r+diag[0.2\quad 0.2\quad 0.2]\,g(e_r)-\begin{bmatrix}19.0964 & 4.3301 & 0 & 0 & 0 & 0\\ 0 & 0 & 19.0964 & 4.3301 & 0 & 0\\ 0 & 0 & 0 & 0 & 19.0964 & 4.3301\end{bmatrix}=0 \quad (43)$$

where $U_{3\times3}$ is a unitary matrix. The initial values of $\hat{W}$ is set to be zero and the adaptation gain Γ is chosen to be 120. Selected results of numerical simulations are shown in the Figure 2 to 11. It has been considered that the spacecraft start with an arbitrary attitude and reach the finial attitude $\beta_f=[0\quad 0\quad 0]^T$ by tracking the following third order reference model with $\nu_m=0.07$:

$$\left[s^3+3\nu_m s^2+3\nu_m^2 s+\nu_m^3\right]\beta_d=0 \quad (44)$$

Smooth control of the attitude was accomplished in the closed-loop system by adaptive estimation of the elements of W. Figure 2 shows that the response time of the desired rigid body rotation is of the order of 15-20 second. Shown in Figure 3 is the resultant of flexural elastic deflections as a function of time and spatial variable x. It is seen that the elastic modes are converging to zero as well. For comparison, residual vibration by using conventional sliding mode is plotted in Figure 4. It can be observed that the use of Hybrid Sliding Surface makes it possible to reduce the residual vibration as well as expedites the error convergence. Convergences of the estimated uncertainties are shown in Figures 5 and 6. The control action history has been plotted in Figure 7.

In order to examine the qualification and robustness of the controller, an external disturbance torque was applied to the hub in other simulation conditions. As shown in

Figures 8,9,10 and 11, the disturbance torque $d(t)=1\ Nm$ was applied between 20 and 30 seconds. Figure 8 shows that the convergence of the tracking error in the new condition was accomplished.

As shown in Figure 9 and 10 the gains have been estimated to a new state by adaptive scheme to reduce the tracking error. Figure 11 shows the variations of the control signals to accommodate disturbance effects.

TABLE 1 NUMERICAL VALUE OF THE SIMULATION PARAMETERS

Parameter	Notation	Value
Appendage length	L	5 m
Appendages stiffness	EI_y	15E3 Kgm^2
	EI_z	5E3 Kgm^2
	GJ_x	15E3 Kgm^2
Mass density of appendages	ρ	2840 Kgm^{-3}
Damping coefficient	μ	0.02
Spacecraft moment of inertia	J	$\begin{bmatrix} 200 & 0 & 0 \\ 0 & 1504 & 0 \\ 0 & 0 & 1501 \end{bmatrix} kgm^2$

Extensive simulations showed that the control system accomplishes large angle rotational maneuvers and vibrations suppression. There are several design parameters which can be properly selected to accomplish rotational maneuver with reasonable control input magnitude and elastic deformation of the beam.

Note that in the proposed control system, sensors and actuators are collocated and mounted on the rigid central body and The measurement of flexible modes is not necessary. So, cost and effort for implementing the control law is low.

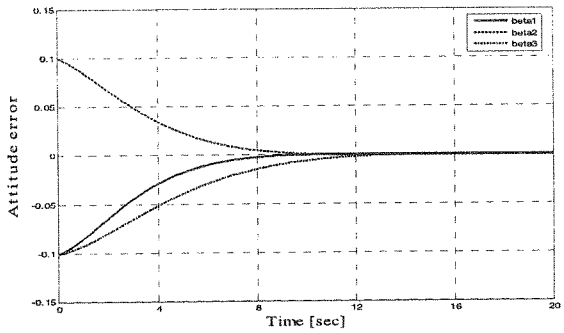

Figure 2: Attitude error.

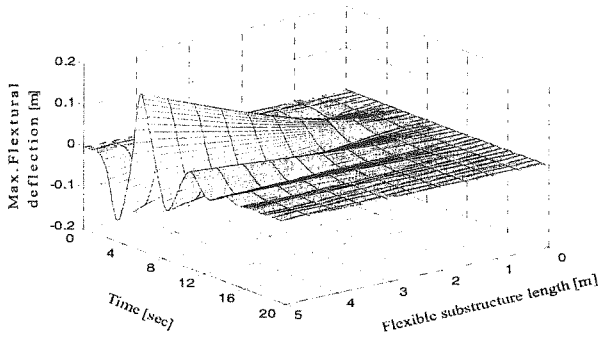

Figure 3: Three dimensional plot for vibration suppression using Hybrid Sliding Mode.

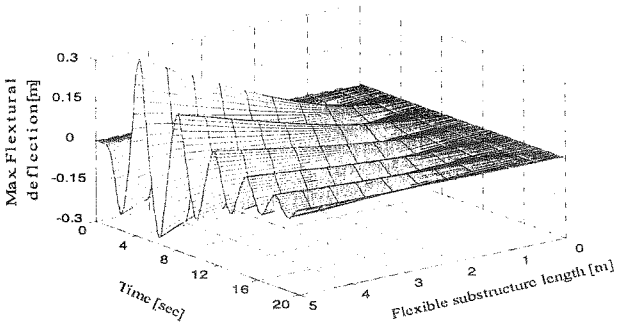

Figure 4: Three dimensional plot for vibration suppression using conventional sliding mode.

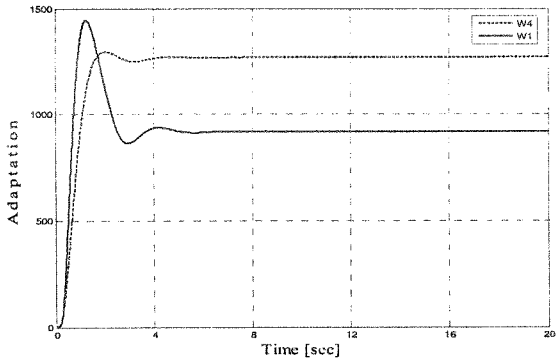

Figure 5: Adaptive estimation of $\|W1\|$ and $\|W4\|$.

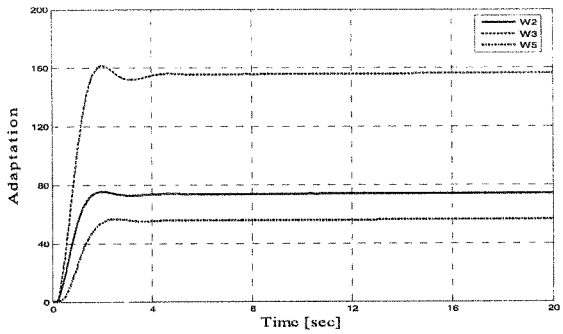

Figure 6: Adaptive estimation of $\|W2\|$, $\|W3\|$ and $\|W5\|$.

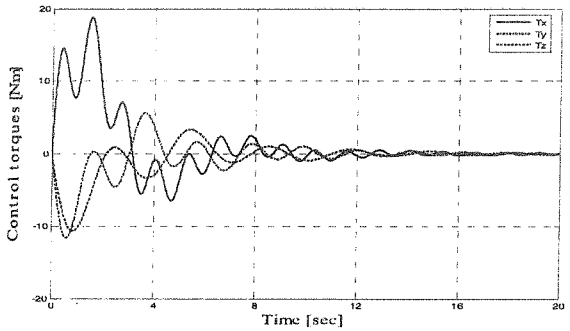

Figure 7: Control actions history.

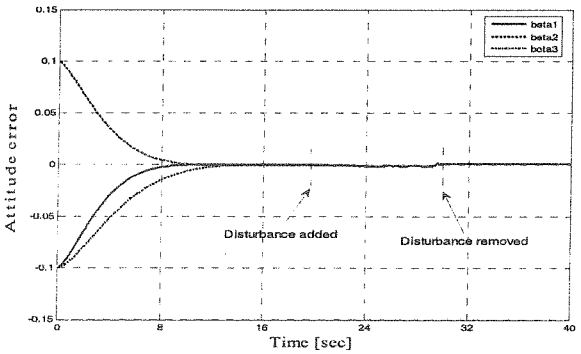

Figure 8: Attitude error with disturbance.

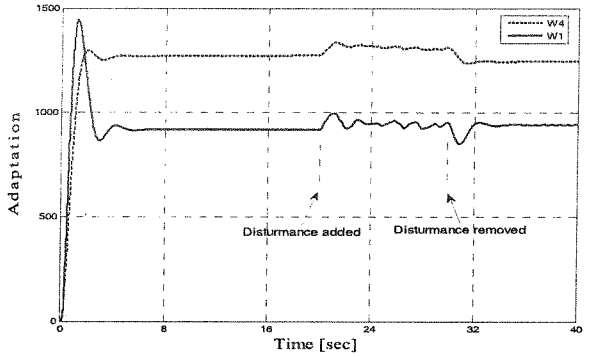

Figure 9: Adaptive estimation of $\|W1\|$ and $\|W4\|$ with disturbance.

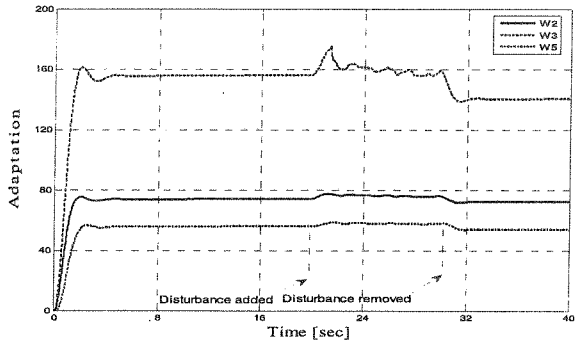

Figure 10: Adaptive estimation of $\|W2\|$, $\|W3\|$ and $\|W5\|$ with disturbance.

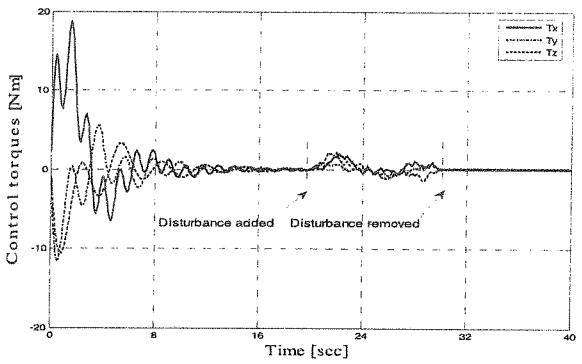

Figure 11: Control actions history with disturbance.

6. CONCLUSION

A robust adaptive control scheme has been developed for multi-axis attitude maneuver of a flexible spacecraft with prescribed configuration. It is based on the adaptive variable structure control scheme with a synthesized hybrid sliding surface. The proposed sliding surface makes it possible to minimize excitation of flexible modes that frequently happen in the conventional sliding mode control, whereas expedites the error convergence near the equilibrium. Using Lyapunov design method, an adaptation law is designed for estimation of the upper bounds of the uncertainties. The adaptation law causes a relativily small gain in the initial stage to reduce the impact to the system and a higher gain at the final stage to lower steady state error. It has been shown that the proposed control and adaptation laws alleviate the difficulties arising from obtaining data for flexible dynamics coordinates, parameter variations and other system uncertainties.

7. APPENDICES

Appendix A: The elements of matrices **M** and **h**

$$\boldsymbol{M}_{rr} = \begin{bmatrix} M_{rr11} & M_{rr12} & M_{rr13} \\ M_{rr21} & M_{rr22} & M_{rr23} \\ M_{rr31} & M_{rr32} & M_{rr33} \end{bmatrix} \tag{A1}$$

$$M_{rr11} = J_{xx} + \sum_{i=1}^{2}\left({}^{i}\boldsymbol{q}_y^T\,{}^{i}N_{yy}\,{}^{i}\boldsymbol{q}_y + {}^{i}\boldsymbol{q}_z^T\,{}^{i}N_{zz}\,{}^{i}\boldsymbol{q}_z + \rho\left({}^{i}a_y^2 + {}^{i}a_z^2\right)\right) + \sum_{i=1}^{2}\left(2\,{}^{i}a_y\,{}^{i}N_y^T\,{}^{i}\boldsymbol{q}_y + 2\,{}^{i}a_z\,{}^{i}N_z^T\,{}^{i}\boldsymbol{q}_z + {}^{i}L\,{}^{i}J_t\right) \tag{A2}$$

$$M_{rr12} = -\sum_{i=1}^{2}\left[{}^{i}N_{yx}^T\,{}^{i}\boldsymbol{q}_y + {}^{i}a_x\,{}^{i}a_y + {}^{i}a_x\,{}^{i}N_y^T\,{}^{i}\boldsymbol{q}_y + \rho\,{}^{i}a_y\,{}^{i}L^2/2\right] \tag{A3}$$

$$M_{rr13} = -\sum_{i=1}^{2}\left[{}^{i}N_{zx}^T\,{}^{i}\boldsymbol{q}_z + {}^{i}a_x\,{}^{i}a_z + {}^{i}a_x\,{}^{i}N_z^T\,{}^{i}\boldsymbol{q}_z + \rho\,{}^{i}a_z\,{}^{i}L^2/2\right] \tag{A4}$$

$$M_{rr21} = -\sum_{i=1}^{2}\left[{}^{i}N_{yx}^T\,{}^{i}\boldsymbol{q}_y + {}^{i}a_x\,{}^{i}a_y + {}^{i}a_x\,{}^{i}N_y^T\,{}^{i}\boldsymbol{q}_y + \rho\,{}^{i}a_y\,{}^{i}L^2/2\right] \tag{A5}$$

$$M_{rr22} = J_{yy} + \sum_{i=1}^{2}\left[{}^{i}q_z^T\, {}^{i}N_{zz}\, {}^{i}q_z + \rho\, {}^{i}a_z^2 + 2\, {}^{i}a_z\, {}^{i}N_z^T\, {}^{i}q_z + \rho \int_0^{L_i} \zeta^2 d\zeta \right] \quad \text{(A6)}$$

$$M_{rr23} = -\sum_{i=1}^{2}\left[{}^{i}q_z^T\, {}^{i}N_{zy}\, {}^{i}q_y + {}^{i}a_y\, {}^{i}a_z + {}^{i}a_y\, {}^{i}N_z^T\, {}^{i}q_z + {}^{i}a_z\, {}^{i}N_y^T\, {}^{i}q_y \right] \quad \text{(A7)}$$

$$M_{rr31} = -\sum_{i=1}^{2}\left[{}^{i}N_{zx}\, {}^{i}q_y + {}^{i}a_y\, {}^{i}a_z + {}^{i}a_y\, {}^{i}N_z^T\, {}^{i}q_z + \rho\, {}^{i}a_z\, {}^{i}L^2/2 \right] \quad \text{(A8)}$$

$$M_{rr32} = -\sum_{i=1}^{2}\left[{}^{i}q_z^T\, {}^{i}N_{zy}\, {}^{i}q_y + {}^{i}a_y\, {}^{i}a_z + {}^{i}a_y\, {}^{i}N_z^T\, {}^{i}q_z + {}^{i}a_z\, {}^{i}N_y^T\, {}^{i}q_y \right] \quad \text{(A9)}$$

$$M_{rr33} = I_{zz} + \sum_{i=1}^{2}\left[{}^{i}q_y^T\, {}^{i}N_{yy}\, {}^{i}q_y + \rho\, {}^{i}a_y^2 + 2\, {}^{i}a_y\, {}^{i}N_y^T\, {}^{i}q_y + \rho \int_0^{L_i} \zeta^2 d\zeta \right] \quad \text{(A10)}$$

$$\boldsymbol{M}_{rf} = \begin{bmatrix} M_{rf11} & M_{rf12} & M_{rf13} \\ M_{rf21} & M_{rf22} & M_{rf23} \\ M_{rf31} & M_{rf32} & M_{rf33} \end{bmatrix} \quad \text{(A11)}$$

$$M_{rf11} = q_y^T \begin{bmatrix} {}^{1}N_{zy} & 0 \\ 0 & {}^{2}N_{zy} \end{bmatrix} + \begin{bmatrix} {}^{1}a_z & {}^{2}a_z \end{bmatrix} \begin{bmatrix} {}^{1}N_y^T & 0 \\ 0 & {}^{2}N_y^T \end{bmatrix} \quad \text{(A12)}$$

$$M_{rf12} = q_y^T \begin{bmatrix} {}^{1}N_{zy} & 0 \\ 0 & {}^{2}N_{zy} \end{bmatrix} + \begin{bmatrix} {}^{1}a_y & {}^{2}a_y \end{bmatrix} \begin{bmatrix} {}^{1}N_z^T & 0 \\ 0 & {}^{2}N_z^T \end{bmatrix} \quad \text{(A13)}$$

$$M_{rf13} = \begin{bmatrix} {}^{1}N_\gamma^T & {}^{2}N_\gamma^T \end{bmatrix} \quad \text{(A14)}$$

$$M_{rf21} = 0 \quad \text{(A15)}$$

$$M_{rf22} = -\begin{bmatrix} {}^{1}N_{zx}^T & {}^{2}N_{zx}^T \end{bmatrix} + \begin{bmatrix} {}^{1}a_x & {}^{2}a_{ox} \end{bmatrix} \begin{bmatrix} {}^{1}N_z^T & 0 \\ 0 & {}^{2}N_z^T \end{bmatrix} \quad \text{(A16)}$$

$$M_{rf23} = 0 \quad \text{(A17)}$$

$$M_{rf31} = -\begin{bmatrix} {}^{1}N_{yx}^T & {}^{2}N_{yx}^T \end{bmatrix} + \begin{bmatrix} {}^{1}a_x & {}^{2}a_x \end{bmatrix} \begin{bmatrix} {}^{1}N_y^T & 0 \\ 0 & {}^{2}N_y^T \end{bmatrix} \quad \text{(A18)}$$

$$M_{rf32} = 0 \quad \text{(A19)}$$

$$M_{rf33} = 0 \quad \text{(A20)}$$

$$\boldsymbol{M}_{fr} = \begin{bmatrix} M_{fr11} & M_{fr12} & M_{fr13} \\ M_{fr21} & M_{fr22} & M_{fr23} \\ M_{fr31} & M_{fr32} & M_{fr33} \end{bmatrix} \quad \text{(A21)}$$

$$M_{fr11} = -\begin{bmatrix} {}^{1}N_{zy} & 0 \\ 0 & {}^{2}N_{zy} \end{bmatrix} {}^{i}q_z + \begin{bmatrix} {}^{1}N_y & 0 \\ 0 & {}^{2}N_y \end{bmatrix} \begin{bmatrix} {}^{1}a_z & {}^{2}a_z \end{bmatrix}^T \quad \text{(A22)}$$

$$M_{fr12} = 0 \quad \text{(A23)}$$

$$M_{fr13} = \begin{bmatrix} {}^{1}N_{yx} \\ {}^{2}N_{yx} \end{bmatrix} + \begin{bmatrix} {}^{1}N_y & 0 \\ 0 & {}^{2}N_y \end{bmatrix} \begin{bmatrix} {}^{1}a_z & {}^{2}a_z \end{bmatrix}^T \quad \text{(A24)}$$

$$M_{fr21} = \begin{bmatrix} {}^{1}N_{zy} & 0 \\ 0 & {}^{2}N_{zy} \end{bmatrix} q_y + \begin{bmatrix} {}^{1}N_z & 0 \\ 0 & {}^{2}N_z \end{bmatrix} \begin{bmatrix} {}^{1}a_y & {}^{2}a_y \end{bmatrix}^T \quad \text{(A25)}$$

$$M_{fr22} = -\begin{bmatrix} {}^{1}N_{zx} \\ {}^{2}N_{zx} \end{bmatrix} + \begin{bmatrix} {}^{1}N_z & 0 \\ 0 & {}^{2}N_z \end{bmatrix} \begin{bmatrix} {}^{1}a_x & {}^{2}a_x \end{bmatrix}^T \quad \text{(A26)}$$

$$M_{fr23} = 0 \quad \text{(A27)}$$

$$M_{fr31} = \begin{bmatrix} {}^{1}N_\gamma & 0 \\ 0 & {}^{2}N_\gamma \end{bmatrix} \begin{bmatrix} {}^{1}J_t & {}^{2}J_t \end{bmatrix}^T \quad \text{(A28)}$$

$$M_{fr32} = 0 \quad \text{(A29)}$$

$$M_{fr33} = 0 \quad \text{(A30)}$$

$$\boldsymbol{M}_{ff} = \begin{bmatrix} M_{ff11} & M_{ff12} & M_{ff13} \\ M_{ff21} & M_{ff22} & M_{ff23} \\ M_{ff31} & M_{ff32} & M_{ff33} \end{bmatrix} \quad \text{(A31)}$$

$$M_{ff11} = \begin{bmatrix} {}^{1}N_{yy} & 0 \\ 0 & {}^{2}N_{yy} \end{bmatrix} \quad \text{(A32)}$$

$$M_{ff12} = 0 \quad \text{(A33)}$$

$$M_{ff13} = 0 \quad \text{(A34)}$$

$$M_{ff21} = 0 \quad \text{(A35)}$$

$$M_{ff22} = \begin{bmatrix} {}^{1}N_{zz} & 0 \\ 0 & {}^{2}N_{zz} \end{bmatrix} \quad \text{(A36)}$$

$$M_{ff23} = 0 \quad \text{(A37)}$$

$$M_{ff31} = 0 \quad \text{(A38)}$$

$$M_{ff32} = 0 \quad \text{(A39)}$$

$$M_{ff33} = \begin{bmatrix} {}^{1}N_{\gamma\gamma} & 0 \\ 0 & {}^{2}N_{\gamma\gamma} \end{bmatrix} \quad \text{(A40)}$$

$$\boldsymbol{h}_r = \begin{bmatrix} h_{r1} & h_{r2} & h_{r3} \end{bmatrix}^T \quad \text{(A41)}$$

$$\begin{aligned} h_{r1} = {} & \omega_y \omega_z \left(J_{zz} - J_{yy} \right) \\ & + \omega_x \omega_y \sum_{i=1}^{2}\left[{}^{i}N_{zx}^T\, {}^{i}q_z + {}^{i}a_x\, {}^{i}a_z + {}^{i}a_x\, {}^{i}N_z^T\, {}^{i}q_z + \rho\, {}^{i}a_z\, {}^{i}L^2/2 \right] \\ & + \omega_x \omega_z \sum_{i=1}^{2}\left[{}^{i}N_{yx}^T\, {}^{i}q_y + {}^{i}a_x\, {}^{i}a_y + {}^{i}a_x\, {}^{i}N_y^T\, {}^{i}q_y + \rho\, {}^{i}a_y\, {}^{i}L^2/2 \right] \\ & + \left(\omega_y^2 - \omega_z^2 \right) \sum_{i=1}^{2}\left[{}^{i}q_z^T\, {}^{i}N_{zy}^T\, {}^{i}q_y + {}^{i}a_y\, {}^{i}a_z + {}^{i}a_y\, {}^{i}N_z^T\, {}^{i}q_z + {}^{i}a_z\, {}^{i}N_y^T\, {}^{i}q_y \right] \\ & + \omega_y \omega_z \sum_{i=1}^{2}\left[{}^{i}q_y^T\, {}^{i}N_{yy}^T\, {}^{i}q_y - {}^{i}q_z^T\, {}^{i}N_{zz}^T\, {}^{i}q_z + \rho\left({}^{i}a_y^2 - {}^{i}a_z^2 \right) \right] \\ & + \omega_y \omega_z \sum_{i=1}^{2}\left[2\rho\, {}^{i}a_y N_y^T\, {}^{i}q_y - 2\rho\, {}^{i}a_z N_z^T\, {}^{i}q_z \right] \\ & + 2\omega_x \sum_{i=1}^{2}\left[{}^{i}q_y^T\, {}^{i}N_{yy}^T\, {}^{i}q_y + {}^{i}a_y\, {}^{i}N_y^T\, {}^{i}\dot{q}_y + {}^{i}q_z^T\, {}^{i}N_{zz}^T\, {}^{i}q_z + {}^{i}a_z\, {}^{i}N_z^T\, {}^{i}\dot{q}_z \right] \end{aligned} \quad \text{(A42)}$$

$$\begin{aligned} h_{r2} = {} & \omega_x \omega_z \left(J_{xx} - J_{yy} \right) \\ & + \omega_z \omega_y \sum_{i=1}^{2}\left[{}^{i}N_{yx}^T\, {}^{i}q_y + {}^{i}a_x\, {}^{i}a_y + {}^{i}a_x\, {}^{i}N_y^T\, {}^{i}q_y + \rho\, {}^{i}a_y\, {}^{i}L^2/2 \right] \\ & + \omega_x \omega_y \sum_{i=1}^{2}\left[{}^{i}q_z^T\, {}^{i}N_{zy}^T\, {}^{i}q_y + {}^{i}a_y\, {}^{i}a_z + {}^{i}a_y\, {}^{i}N_z^T\, {}^{i}q_z + {}^{i}a_z\, {}^{i}N_y^T\, {}^{i}q_y \right] \\ & + \left(\omega_x^2 - \omega_z^2 \right) \sum_{i=1}^{2}\left[{}^{i}N_{zx}^T\, {}^{i}q_z + {}^{i}a_x\, {}^{i}a_z + {}^{i}a_x\, {}^{i}N_z^T\, {}^{i}q_z + \rho\, {}^{i}a_z\, {}^{i}L^2/2 \right] \\ & + \omega_z \omega_x \sum_{i=1}^{2}\left[{}^{i}q_z^T\, {}^{i}N_{zz}^T\, {}^{i}q_z + \rho\, {}^{i}a_z^2 + 2\, {}^{i}a_z N_z^T\, {}^{i}q_z + {}^{i}L\, {}^{i}J_t/2 \right] \\ & - 2\omega_x \sum_{i=1}^{2}\left[{}^{i}N_{yx}^T\, {}^{i}\dot{q}_y + {}^{i}a_x\, {}^{i}N_y^T\, {}^{i}\dot{q}_y \right] \\ & + 2\omega_y \sum_{i=1}^{2}\left[{}^{i}q_z^T\, {}^{i}N_{zz}^T\, {}^{i}\dot{q}_z + {}^{i}a_z\, {}^{i}N_z^T\, {}^{i}\dot{q}_z \right] \\ & - 2\omega_z \sum_{i=1}^{2}\left[{}^{i}q_z^T\, {}^{i}N_{zy}^T\, {}^{i}\dot{q}_y + {}^{i}a_z\, {}^{i}N_y^T\, {}^{i}\dot{q}_y - {}^{i}N_\gamma^T\, {}^{i}\dot{q}_\gamma/2 \right] \end{aligned} \quad \text{(A43)}$$

$$\begin{aligned} h_{r3} = {} & \omega_y \omega_x \left(J_{yy} - J_{xx} \right) \\ & + \omega_y \omega_z \sum_{i=1}^{2}\left[{}^{i}N_{zx}^T\, {}^{i}q_z + {}^{i}a_x\, {}^{i}a_z + {}^{i}a_x\, {}^{i}N_z^T\, {}^{i}q_z + \rho\, {}^{i}a_z\, {}^{i}L^2/2 \right] \end{aligned}$$

$$-\omega_x\omega_y\sum_{i=1}^{2}\left[{}^iq_z^T\,{}^iN_{zz}^T\,{}^iq_z+{}^ia_y\,{}^ia_z+{}^ia_y\,{}^iN_z^T\,{}^iq_z+{}^ia_z\,{}^iN_y^T\,{}^iq_y\right]$$

$$-\left(\omega_x^2-\omega_y^2\right)\sum_{i=1}^{2}\left[{}^iN_{yx}^T\,{}^iq_y+{}^ia_x\,{}^ia_y+{}^ia_x\,{}^iN_y^T\,{}^iq_y+\rho\,{}^ia_y\,{}^iL^2/2\right]$$

$$-\omega_x\omega_y\sum_{i=1}^{2}\left[{}^iq_y^T\,{}^iN_{yy}^T\,{}^iq_y+\rho\,{}^ia_y^2+2\,{}^ia_yN_y^T\,{}^iq_y+{}^iL\,{}^iJ_t/2\right]$$

$$-2\omega_x\sum_{i=1}^{2}\left[{}^iN_{zx}^T\,{}^i\dot{q}_z+{}^ia_x\,{}^iN_z^T\,{}^i\dot{q}_z\right]$$

$$-2\omega_y\sum_{i=1}^{2}\left[{}^i\dot{q}_z^T\,{}^iN_{zy}^T\,{}^iq_y+{}^ia_y\,{}^iN_z^T\,{}^i\dot{q}_z+{}^iN_\gamma^T\,{}^i\dot{q}_\gamma/2\right]$$

$$+2\omega_z\sum_{i=1}^{2}\left[{}^i\dot{q}_y^T\,{}^iN_{yy}^T\,{}^iq_y+{}^ia_y\,{}^iN_y^T\,{}^i\dot{q}_y\right] \tag{A44}$$

$$\boldsymbol{h}_f=\begin{bmatrix}\boldsymbol{h}_{f1} & \boldsymbol{h}_{f2} & \boldsymbol{h}_{f3}\end{bmatrix}^T \tag{A45}$$

$$\begin{aligned}h_{f1}=&-\left(\omega_x^2+\omega_z^2\right)\left(\begin{bmatrix}{}^1N_{yy} & 0\\ 0 & {}^2N_{yy}\end{bmatrix}q_y+\begin{bmatrix}{}^1N_y & 0\\ 0 & {}^2N_y\end{bmatrix}\begin{bmatrix}{}^1a_y & {}^2a_y\end{bmatrix}^T\right)\\&+\omega_y\omega_x\left(\begin{bmatrix}{}^1N_{xy}\\ {}^2N_{xy}\end{bmatrix}+\begin{bmatrix}{}^1N_y & 0\\ 0 & {}^2N_y\end{bmatrix}\begin{bmatrix}{}^1a_x & {}^2a_x\end{bmatrix}^T\right)\\&+\omega_y\omega_z\left(\begin{bmatrix}{}^1N_{yz} & 0\\ 0 & {}^2N_{yz}\end{bmatrix}q_z+\begin{bmatrix}{}^1N_z & 0\\ 0 & {}^2N_z\end{bmatrix}\begin{bmatrix}{}^1a_z & {}^2a_z\end{bmatrix}^T\right)\\&-2\omega_x\left(\begin{bmatrix}{}^1N_{yz} & 0\\ 0 & {}^2N_{yz}\end{bmatrix}\dot{q}_z\right)+\left(\begin{bmatrix}{}^1Q_{yy} & 0\\ 0 & {}^2Q_{yy}\end{bmatrix}q_y\right)\end{aligned} \tag{A46}$$

$$\begin{aligned}h_{f2}=&-\left(\omega_x^2+\omega_y^2\right)\left(\begin{bmatrix}{}^1N_{zz} & 0\\ 0 & {}^2N_{zz}\end{bmatrix}q_z+\begin{bmatrix}{}^1N_z & 0\\ 0 & {}^2N_z\end{bmatrix}\begin{bmatrix}{}^1a_z & {}^2a_z\end{bmatrix}^T\right)\\&+\omega_x\omega_z\left(\begin{bmatrix}{}^1N_{xy}\\ {}^2N_{xy}\end{bmatrix}+\begin{bmatrix}{}^1N_z & 0\\ 0 & {}^2N_z\end{bmatrix}\begin{bmatrix}{}^1a_x & {}^2a_x\end{bmatrix}^T\right)\\&+\omega_y\omega_z\left(\begin{bmatrix}{}^1N_{yz} & 0\\ 0 & {}^2N_{yz}\end{bmatrix}q_y+\begin{bmatrix}{}^1N_z & 0\\ 0 & {}^2N_z\end{bmatrix}\begin{bmatrix}{}^1a_y & {}^2a_y\end{bmatrix}^T\right)\\&-2\omega_x\left(\begin{bmatrix}{}^1N_{yz} & 0\\ 0 & {}^2N_{yz}\end{bmatrix}\dot{q}_y\right)+\left(\begin{bmatrix}{}^1Q_{zz} & 0\\ 0 & {}^2Q_{zz}\end{bmatrix}q_z\right)\end{aligned} \tag{A47}$$

$$h_{f3}=-\begin{bmatrix}{}^1Q_{\gamma\gamma} & 0\\ 0 & {}^2Q_{\gamma\gamma}\end{bmatrix}q_\gamma \tag{A48}$$

$${}^iN_{yy}=\int_0^{L_i}\rho\,{}^i\Psi_y(\zeta)\,{}^i\Psi_y^T(\zeta)d\zeta \tag{A49}$$

$${}^iN_y=\int_0^{L_i}\rho\,{}^i\Psi_y(\zeta)d\zeta \tag{A50}$$

$${}^iN_{zz}=\int_0^{L_i}\rho\,{}^i\Psi_z(\zeta)\,{}^i\Psi_z^T(\zeta)d\zeta \tag{A51}$$

$${}^iN_z=\int_0^{L_i}\rho\,{}^i\Psi_z(\zeta)d\zeta \tag{A52}$$

$${}^iN_{yx}=\int_0^{L_i}\rho\,{}^i\Psi_y(\zeta)\zeta\,d\zeta \tag{A53}$$

$${}^iN_{zy}=\int_0^{L_i}\rho\,{}^i\Psi_z(\zeta)\,{}^i\Psi_y^T(\zeta)d\zeta \tag{A54}$$

$${}^iN_{zx}=\int_0^{L_i}\rho\,{}^i\Psi_z(\zeta)\zeta\,d\zeta \tag{A55}$$

$${}^iN_\gamma=\int_0^{L_i}{}^iJ_t\;{}^i\Psi_\gamma^T(\zeta)d\zeta \tag{A56}$$

$${}^iN_{\gamma\gamma}=\int_0^{L_i}{}^iJ_t\;{}^i\Psi_\gamma(\zeta)\,{}^i\Psi_\gamma^T(\zeta)d\zeta \tag{A57}$$

$${}^iQ_{yy}=\int_0^{L_i}{}^i(EI)_y\;{}^i\Psi_y(\zeta)\frac{d^4}{dx^4}\left({}^i\Psi_y(\zeta)\right)d\zeta \tag{A58}$$

$${}^iQ_{zz}=\int_0^{L_i}{}^i(EI)_z\;{}^i\Psi_z(\zeta)\frac{d^4}{dx^4}\left({}^i\Psi_z(\zeta)\right)d\zeta \tag{A59}$$

$${}^iQ_{\gamma\gamma}=\int_0^{L_i}{}^i(GJ)_x\;{}^i\Psi_\gamma(\zeta)\frac{d^2}{dx^2}\left({}^i\Psi_\gamma(\zeta)\right)d\zeta \tag{A60}$$

${}^i\Psi_{(\_)}(\zeta)$ are the shape function vectors for elastic deformations of the ith flexible substructure, ${}^ia_x$, ${}^ia_y$ and ${}^ia_z$ are the coordinates of ith flexible substructure attachment point in x, y and z directions, respectively and J_t is torsional moment of inertia.

Appendix b: The elements of matrix Y

$$Y1=\begin{bmatrix}\omega_x & \omega_y & \omega_z & \omega_x\omega_y & \omega_x\omega_z & \omega_y\omega_z & \omega_x^2-\omega_y^2 & \omega_y^2-\omega_z^2 & \omega_x^2-\omega_z^2\end{bmatrix} \tag{B1}$$

$$Y2=e_r \tag{B2}$$

$$Y3=\dot{g}(e_r) \tag{B3}$$

$$Y4=z \tag{B4}$$

$$Y5=\begin{bmatrix}1 & 1 & 1\end{bmatrix}^T \tag{B5}$$

8. References

[1] D. C. Hyland, J. L. Junkins and R. W Longman, Active Control Technology for Space Structure, Journal of Guidance, Control and Dynamics, Vol. 16, No. 5, 801-821, (1993).

[2] R. M. Byers, S. R. Vadali and J. L. Junkins, Near-Minimum Time Closed-Loop Slewing of Flexible Spacecraft, Journal of Guidance, Control and Dynamics, Vol. 13, No. 1, 57-65, (1990).

[3] J. Ben-Asher, J. A. Burns and E. M. Cliff, Time Optimal Slewing of Flexible Structure, Journal of Guidance, Control and Dynamics, Vol. 15, No.1, 360-367, (1992).

[4] J. L. Junkins and H. Bang, Maneuver and Vibration Control of Hybrid Coordinate Systems Using Lyapunov Stability Theory, Journal of Guidance, Control and Dynamics, Vol. 16, No. 4, 665-676, (1993).

[5] J. Suk, S. Boo and Y. Kim, Lyapunov Control Law for Slew Maneuver Using Time Finite Element Analysis, Journal of Guidance, Control and Dynamics, Vol. 24, No. 1, 87-94, (2001).

[6] Y. Y. Lin and G. L. Lin, General Attitude Maneuvers of Spacecraft with Flexible Structures, Journal of Guidance, Control and Dynamics, Vol. 18, No. 2, 264-171, (1995).

[7] D. Gorinevsky and G. Vukovich, Nonlinear Input Shaping Control of Flexible Spacecraft Reorient- ation Maneuver, Journal of Guidance, Control and Dynamics, Vol. 21, No. 2, 264-270, (1998).

[8] G. Song, N. Buck and B. Agrawal, Spacecraft Vibration Reduction Using Pulse-Width Pulse- Frequency Modulated Input Shaper, Journal of Guidance, Control and Dynamics, Vol. 22, No. 3, 433-440, (1999).

[9] W. H. Bennett, C. LaVigna, H. G. Kwatny and G. Blankenship, Nonlinear and Adaptive Control of Flexible Space Structure,

Journal of Dynamic Systems, Measurement and Control, Vol. 115, 86-94, (1993).
[10] S. N. Singh and A. D. De Araujo, Adaptive Control and Stabilization of Elastic Spacecraft, IEEE Transactions on Aerospace and Electronic Systems, Vol. 35, No.1, 115-121, (1999).
[11] A. M. Annaswamy and D. J. Clancy, Adaptive Control Strategies for Flexible Space Structures, IEEE Transactions on Aerospace and Electronic Systems, Vol.32, No. 3, 952-965, (1996).
[12] A. Iyer and S. N. Singh, Variable Structure Slewing Control and Vibration Damping of Flexible Space Structure, Acta Astronautica, Vol. 25, No. 1, 1-9, (1991).
[13] S. S. Ge, T. H. Lee and F. Hong, Variable Structure Maneuvering Control of a Flexible Spacecraft, Proceedings of the American Control Conference, Arlington, VA, 1599-1604, (2001).
[14] F. Karray, A. Grewal, M. Glaum and V. Modi, Stiffening Control of a Class of Nonlinear Affine Systems, IEEE Transactions on Aerospace and Electronic Systems, Vol.33, No.2, (1997).
[15] Shahravi, M. and Kabganian, M., Slewing Control of Flexible Space Structures, Proceeding of the 7th International Conference in Mechanical Engineering (ISME2003), Mashad, Iran, 506-511, (2003).
[16] J. X. Xu, and W. J. Cao, Synthesized Sliding Mode Control of a Single-Link Flexible Robot, International Journal of Control, Vol.73, No.3, 197-209, (2000).
[17] K. D. Young and U. Ozguner, Frequency Shaping Compensator Design for Sliding Mode, International Journal of Control, Vol.57, 1005-1019, (1993).
[18] M. Zak, Terminal Attractors for Addressable Memory in Neural Network, Physics Letters A, Vol.133, 18-22 (1988).
[19] Slotine, J. J. E., and Li, W., Applied Nonlinear Control, Prentice-Hall, NJ, (1991).